

Electronic Supplementary Information

Experimental Section

Materials: Boric acid (H_3BO_3), *p*-dimethylaminobenzaldehyde ($p\text{-C}_9\text{H}_{11}\text{NO}$), hydrazine hydrate ($\text{N}_2\text{H}_4\cdot\text{H}_2\text{O}$), H_2O_2 (30 wt%), and Nafion (5 wt%) were purchased from Sigma-Aldrich Chemical Reagent Co., Ltd.. Urea ($\text{CO}(\text{NH}_2)_2$), salicylate sodium ($\text{Na}_3\text{C}_6\text{H}_5\text{O}_7$), sodium hypochlorite (NaClO), and sodium nitroferricyanide ($\text{Na}_2[\text{Fe}(\text{CN})_5\text{NO}]_2\cdot\text{H}_2\text{O}$) were brought from Tianjin Fuyu Chemical Reagent Co. Ltd.. Sulfuric acid (H_2SO_4), hydrochloric acid (HCl) and ethanol ($\text{C}_2\text{H}_5\text{OH}$) were purchased from Chengdu Kelong Chemical Reagent Factory. Nafion 117 membrane (DuPont) was purchased from HESEN Co., Ltd.. The water used throughout all experiments was purified through a Millipore system. All reagents were used as received without further purification.

Preparation of MBN and BBN: In a typical synthesis,¹ $\text{CO}(\text{NH}_2)_2$ (9.00 g) and H_3BO_3 (1.85 g) were dissolved in deionized water (450 mL) at 65 °C, and water was then allowed to completely evaporate at that temperature. The intermediates were ground and loaded in an alumina boat crucible and then heated in a tubular furnace under N_2 atmosphere from room temperature to 1050 °C at a rate of 10 °C min^{-1} . This temperature was maintained for 3.5 h. The samples were allowed to cool to ambient temperature while maintaining the same nitrogen flow. At the end of the synthesis, a white powder (MBN) was obtained. The BBN was prepared by drying in the oven at 65 °C for 24 h before heated in a tubular furnace.

Preparation of MBN/CP electrode: The MBN ink was prepared by dispersing 5 mg of MBN catalyst dispersed into 1 mL ethanol containing 20 μL of 5 wt% Nafion and kept ultrasonic for 1 h. Then 40 μL of the MBN ink was loaded on the carbon paper (1 cm \times 1 cm). The MBN/CP working electrode was prepared well.

Characterizations

XRD patterns were obtained from a Shimadzu XRD-6100 diffractometer with Cu K α radiation (40 kV, 30 mA) of wavelength 0.154 nm (Japan). SEM images were collected from the tungsten lamp-equipped SU3500 scanning electron microscope at an accelerating voltage of 20 kV (HITACHI, Japan). TEM images were obtained from a Zeiss Libra 200FE transmission electron microscope operated at 200 kV. XPS measurements were performed on an ESCALABMK II X-ray photoelectron spectrometer using Mg as the exciting source. The absorbance data of spectrophotometer were measured on SHIMADZU UV-2700 ultraviolet-visible (UV-Vis) spectrophotometer.

Electrochemical measurements: Before NRR measures, Nafion 211 membrane was pre-treated by heating in 5% H₂O₂ solution and ultrapure water at 80 °C for 1 h, respectively. Electrochemical measurements were performed with a CHI 660D electrochemical analyzer (CH Instruments, Inc., Shanghai) in a standard three-electrode system using MBN/CP (1.0 cm \times 1.0 cm) as the working electrode, a graphite rod as the counter electrode and an Ag/AgCl electrode as the reference electrode. Electrochemical characterization of the MBN/CP catalysts was carried out in 0.1 M Na₂SO₄ electrolytes. All experiments were carried out at room temperature (25 °C). For N₂ reduction experiments, the electrolyte was bubbled with N₂ for 30 min before the measurement. All potentials measured were calibrated to RHE using the following equation:

$$E_{\text{RHE}} = E_{\text{Ag/AgCl}} + 0.059 \times \text{pH} + E^{\circ}_{\text{Ag/AgCl}} \quad (\text{E-1})$$

Determination of NH₃: The produced ammonia was estimated by indophenol blue method by ultraviolet spectroscopy.² In detail, 4 mL electrolyte was removed from the cathodic chamber and added into 50 μ L oxidizing solution containing NaClO ($\rho_{\text{Cl}} = 4\text{--}4.9$) and NaOH (0.75 M), followed by further adding 500 μ L coloring solution

containing 0.4 M $C_7H_5O_3Na$ and 0.32 M NaOH, and 50 μ L catalyst solution (0.1 g $Na_2[Fe(CN)_5NO] \cdot H_2O$ diluted to 10 mL with deionized water) in turn. After standing at 25 °C for 2 h, the UV-Vis absorption spectrum was measured. The concentration of indophenol blue was determined using the absorbance at a wavelength of 655 nm. The concentration-absorbance curve was calibrated using standard ammonia chloride solution with a series of concentrations. The fitting curve ($y = 0.373x + 0.010$, $R^2 = 0.999$) shows good linear relation of absorbance value with NH_4^+ concentration by three times independent calibrations.

Determination of N_2H_4 : The N_2H_4 present in the electrolyte was determined by the method of Watt and Chrisp.³ The *p*- $C_9H_{11}NO$ (5.99 g), HCl (30 mL), and C_2H_5OH (300 mL) were mixed and used as a color reagent. In detail, 5 mL electrolyte was removed from the electrochemical reaction vessel, and added into 5 mL prepared color reagent and stirred 15 min at 25 °C. The obtained calibration curve of N_2H_4 is $y = 1.364x + 0.014$, $R^2 = 0.999$.

Calculations of R_{NH_3} and FE: R_{NH_3} was calculated using the following equation:

$$R_{NH_3} (\mu g h^{-1} mg_{cat.}^{-1}) = ([NH_3] \times V) / (17 \times t \times m_{cat.}) \quad (E-2)$$

Where $[NH_3]$ ($\mu g mL^{-1}$) is the measured NH_3 concentration; V (mL) is the volume of electrolyte; t (h) is the reaction time; m (mg) is the mass loading of catalyst on CP.

FE was calculated according to following equation:

$$FE = 3 \times F \times [NH_3] \times V / (17 \times Q) \quad (E-3)$$

Where F is the Faraday constant ($96500 C mol^{-1}$); and Q (C) is the quantity of applied electricity.

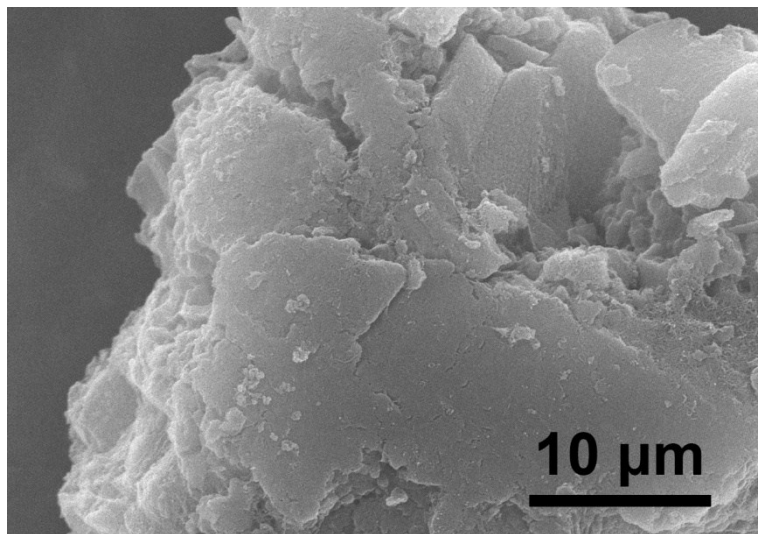


Fig. S1. SEM image of BBN.

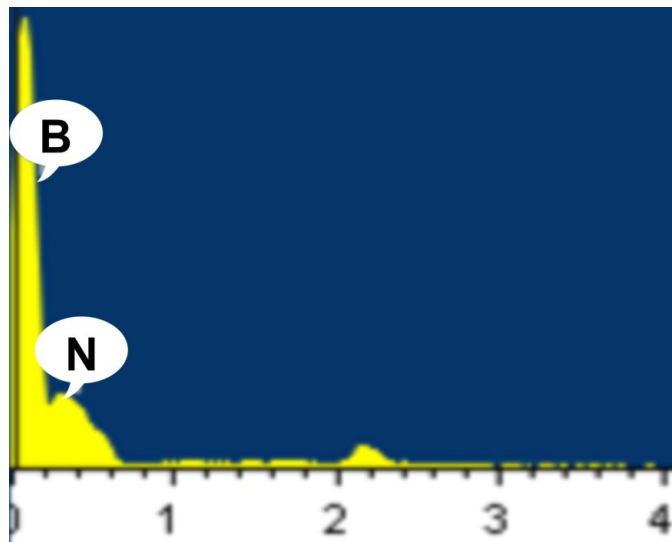


Fig. S2. EDX spectrum of MBN.

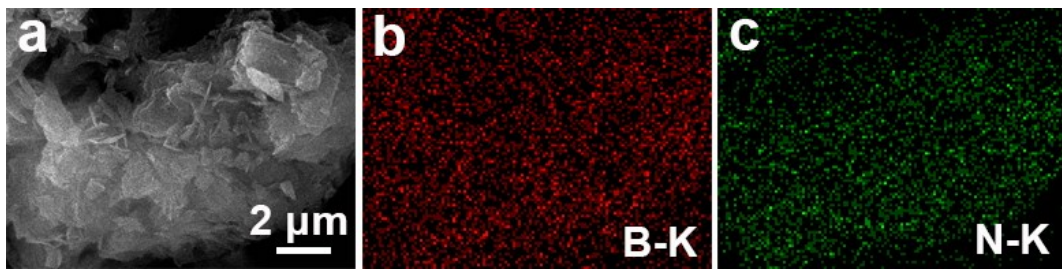


Fig. S3. (a) SEM and EDX elemental mapping images of (b) B and (c) N elements in MBN.

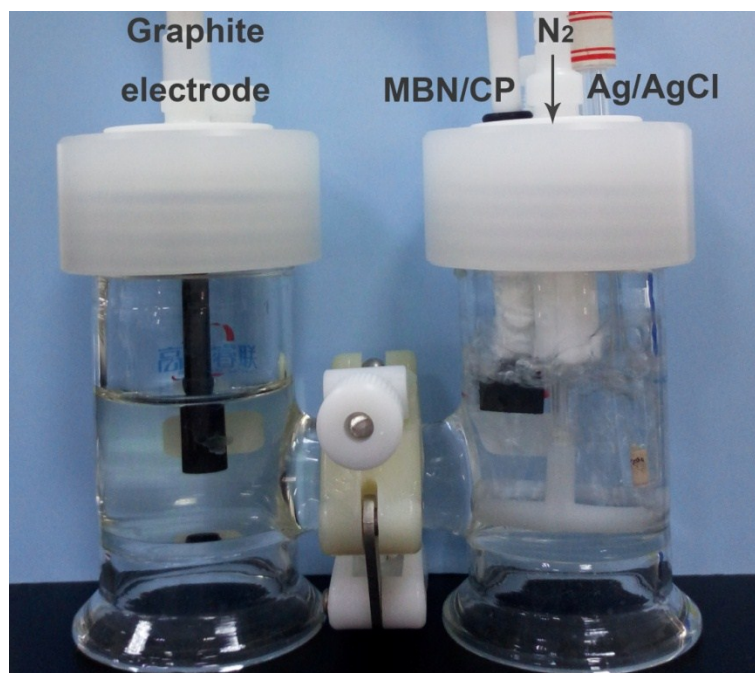


Fig. S4. Optical photograph of the reactor.

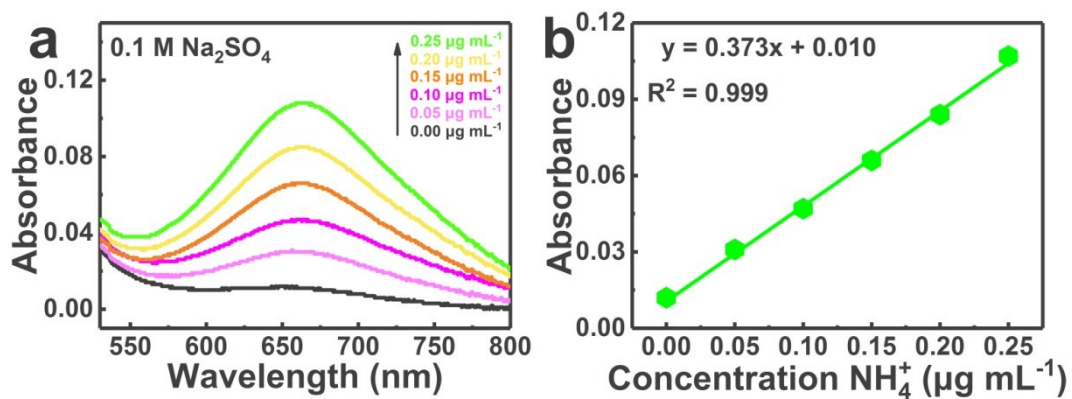


Fig. S5. (a) UV-Vis absorption spectra of indophenol assays with different NH_4^+ concentrations after incubated for 2 h at room temperature. (b) Calibration curve used for calculation of NH_4^+ concentrations.

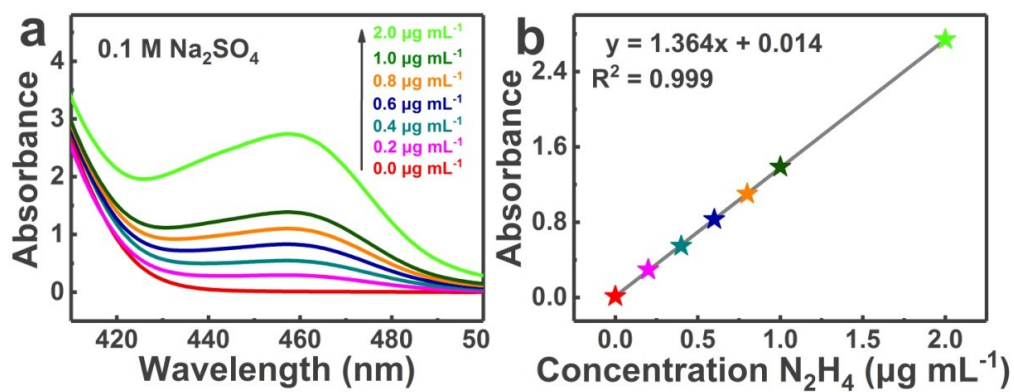


Fig. S6. UV-Vis absorption spectra of various N_2H_4 concentrations after incubated for 10 min at room temperature. (b) Calibration curve used for calculation of N_2H_4 concentrations.

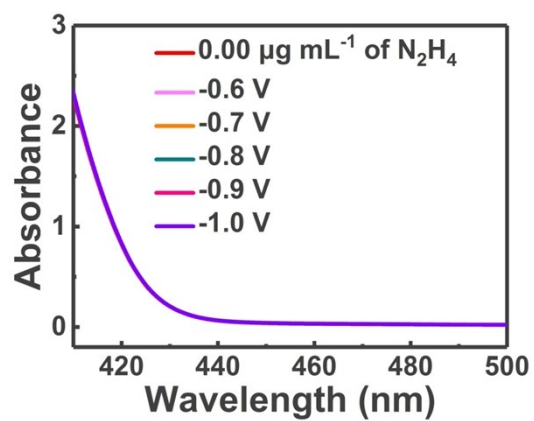


Fig. S7. UV-Vis absorption spectra of the electrolytes stained with *p*-C₉H₁₁NO indicator after NRR electrolysis at a series of potentials.

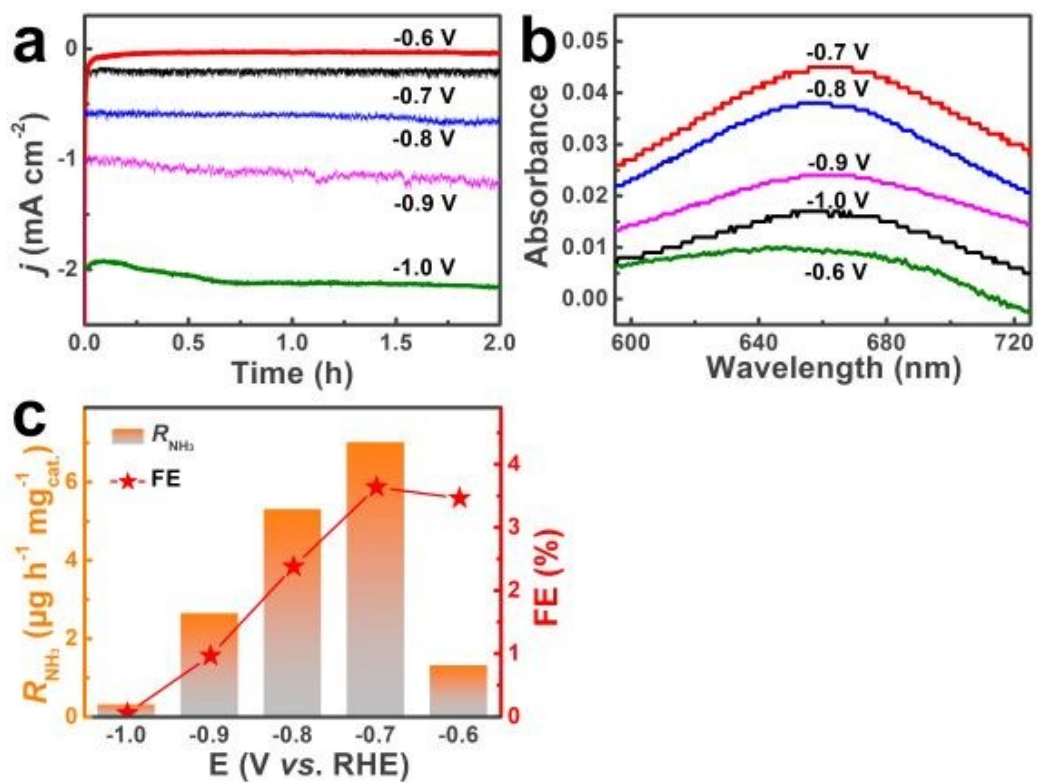


Fig. S8. (a) Chronoamperometry curves of BBN/CP in 0.1 M Na₂SO₄ solution at different potentials. (b) UV-Vis absorption spectra of the electrolytes stained with indophenol indicator after NRR electrolysis at different potentials for 2 h. (c) R_{NH_3} and corresponding FEs of BBN/CP for NRR at different potentials.

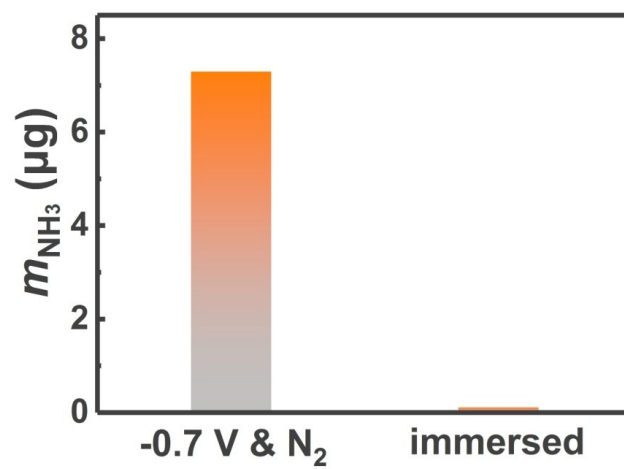


Fig. S9. m_{NH_3} for MBN/CP at different test conditions.

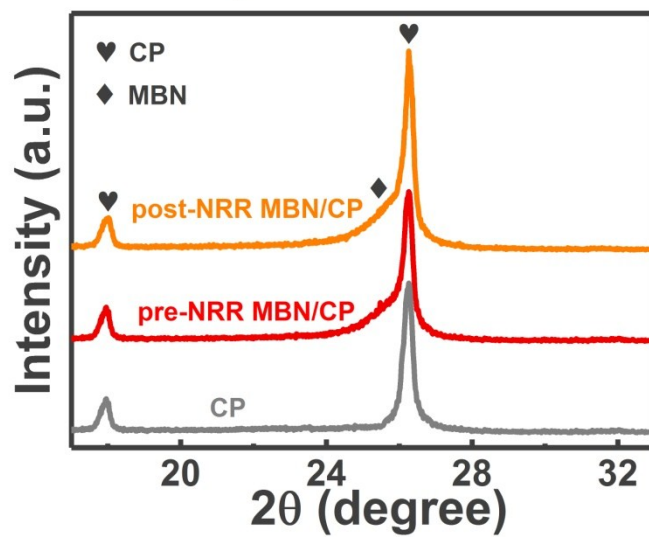


Fig. S10. XRD patterns of bare CP, MBN/CP and post-NRR MBN/CP.

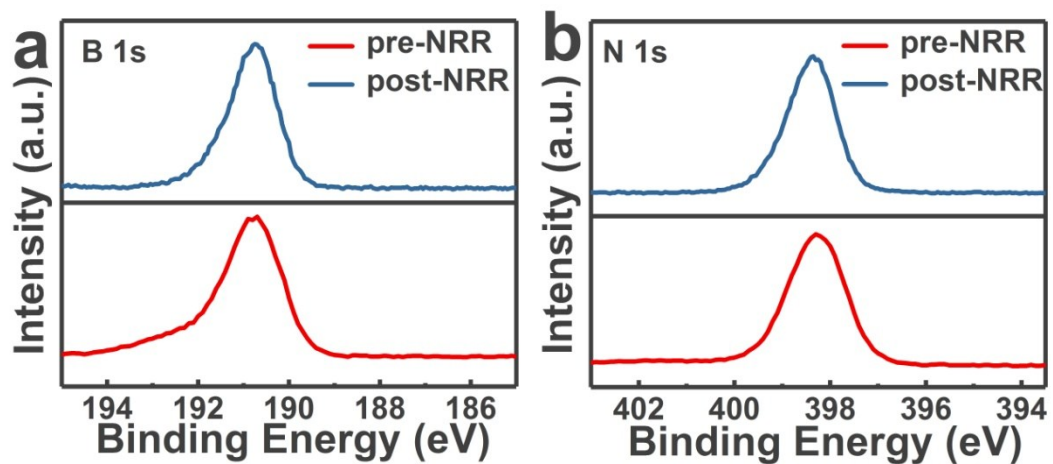


Fig. S11. XPS spectra of MBN in the (a) B 1s and (b) N 1s regions pre- and post-NRR.

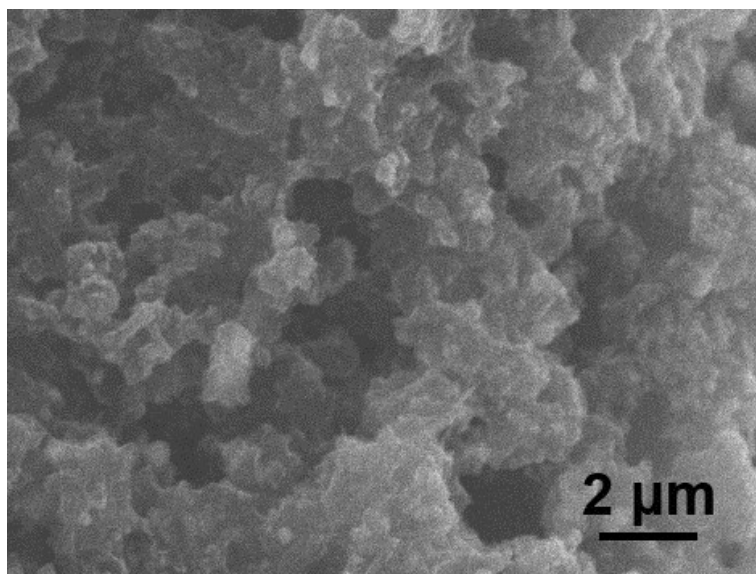


Fig. S12. SEM image of MBN post-NRR.

Table S1. Comparison of the NH₃ electrosynthesis activity for MBN/CP with other aqueous-based NRR electrocatalysts at ambient conditions.

Catalyst	Electrolyte	R_{NH_3}	FE (%)	Ref.
MBN/CP	0.1 M Na₂SO₄	18.2 $\mu\text{g h}^{-1} \text{mg}_{\text{cat.}}^{-1}$	5.5	This work
$\gamma\text{-Fe}_2\text{O}_3$	0.1 M KOH	0.212 $\mu\text{g h}^{-1} \text{mg}_{\text{cat.}}^{-1}$	1.9	4
Fe ₂ O ₃ -CNT	0.1 M KHCO ₃	0.22 $\mu\text{g h}^{-1} \text{cm}_{\text{cat.}}^{-2}$	0.15	5
Fe ₃ O ₄ /Ti	0.1 M Na ₂ SO ₄	3.43 $\mu\text{g h}^{-1} \text{cm}_{\text{cat.}}^{-2}$	2.60	6
Mo nanofilm	0.01 M H ₂ SO ₄	1.89 $\mu\text{g h}^{-1} \text{cm}_{\text{cat.}}^{-2}$	0.72	7
MoO ₃	0.1 M HCl	29.43 $\mu\text{g h}^{-1} \text{mg}_{\text{cat.}}^{-1}$	1.9	8
MoS ₂ /CC	0.1 M Na ₂ SO ₄	4.94 $\mu\text{g h}^{-1} \text{cm}_{\text{cat.}}^{-2}$	1.17	9
Mo ₂ N	0.1 M HCl	78.4 $\mu\text{g h}^{-1} \text{mg}_{\text{cat.}}^{-1}$	4.5	10
MoN	0.1 M HCl	18.42 $\mu\text{g h}^{-1} \text{cm}_{\text{cat.}}^{-2}$	1.15	11
VN	0.1 M HCl	5.14 $\mu\text{g h}^{-1} \text{cm}_{\text{cat.}}^{-2}$	2.25	12
Au NRs	0.1 M KOH	1.64 $\mu\text{g h}^{-1} \text{cm}_{\text{cat.}}^{-2}$	3.88	13
a-Au/CeO _x -RGO	0.1 M HCl	8.3 $\mu\text{g h}^{-1} \text{mg}_{\text{cat.}}^{-1}$	10.1	14
TA-reduced Au/TiO ₂	0.1 M HCl	21.4 $\mu\text{g h}^{-1} \text{mg}_{\text{cat.}}^{-1}$	8.11	15
Pd/C	0.1 M PBS	4.5 $\mu\text{g h}^{-1} \text{mg}_{\text{cat.}}^{-1}$	8.2	16
Pd _{0.2} Cu _{0.8} /rGO	0.1 M KOH	2.80 $\mu\text{g h}^{-1} \text{mg}_{\text{cat.}}^{-1}$	4.5	17
carbon nitride	0.1 M HCl	8.09 $\mu\text{g h}^{-1} \text{mg}_{\text{cat.}}^{-1}$	11.59	18
PCN	0.05 M H ₂ SO ₄	27.2 $\mu\text{g h}^{-1} \text{mg}_{\text{cat.}}^{-1}$	1.42	19
N-doped porous carbon	0.1 M HCl	15.7 $\mu\text{g h}^{-1} \text{mg}_{\text{cat.}}^{-1}$	1.45	20
hollow Cr ₂ O ₃ microspheres	0.1 M Na ₂ SO ₄	25.3 $\mu\text{g h}^{-1} \text{mg}_{\text{cat.}}^{-1}$	6.78	21

TiO ₂ -rGO	0.1 M Na ₂ SO ₄	15.13 $\mu\text{g h}^{-1} \text{mg}_{\text{cat.}}^{-1}$	3.3	22
Nb ₂ O ₅ nanofiber	0.1 M HCl	43.6 $\mu\text{g h}^{-1} \text{mg}_{\text{cat.}}^{-1}$	9.26	23
defect-rich MoS ₂ nanoflower	0.1 M Na ₂ SO ₄	29.28 $\mu\text{g h}^{-1} \text{mg}_{\text{cat.}}^{-1}$	8.34	24
B ₄ C	0.1 M HCl	26.57 $\mu\text{g h}^{-1} \text{mg}_{\text{cat.}}^{-1}$	15.95	25
VO ₂ hollow microsphere	0.1 M Na ₂ SO ₄	14.85 $\mu\text{g h}^{-1} \text{mg}_{\text{cat.}}^{-1}$	3.97	26
Ti ₃ C ₂ T _x nanosheet	0.1 M HCl	20.4 $\mu\text{g h}^{-1} \text{mg}_{\text{cat.}}^{-1}$	9.3	27
Mo ₂ C nanorod	0.1 M HCl	95.1 $\mu\text{g h}^{-1} \text{mg}_{\text{cat.}}^{-1}$	8.13	28
V ₂ O ₃ /C	0.1 M Na ₂ SO ₄	12.3 $\mu\text{g h}^{-1} \text{mg}_{\text{cat.}}^{-1}$	7.28	29
oxygen-doped carbon nanosheet	0.1 M HCl	20.15 $\mu\text{g h}^{-1} \text{mg}_{\text{cat.}}^{-1}$	4.97	30

References:

1. S. Marchesini, A. Regoutz, D. Payne and C. Petit, *Micropor. Mesopor. Mat.*, 2017, **243**, 154–163.
2. D. Zhu, L. Zhang, R. E. Ruther and R. J. Hamers, *Nat. Mater.*, 2013, **12**, 836–841.
3. G. W. Watt and J. D. Chrisp, *Anal. Chem.*, 1952, **24**, 2006–2008.
4. J. Kong, A. Lim, C. Yoon, J. H. Jang, H. C. Ham, J. Han, S. Nam, D. Kim, Y. Sung, J. Choi and H. S. Park, *ACS Sustainable Chem. Eng.*, 2017, **5**, 10986–10995.
5. S. Chen, S. Perathoner, C. Ampelli, C. Mebrahtu, D. Su and G. Centi, *Angew. Chem., Int. Ed.*, 2017, **56**, 2699–2703.
6. Q. Liu, X. Zhang, B. Zhang, Y. Luo, G. Cui, F. Xie and X. Sun, *Nanoscale*, 2018, **10**, 14386–14389.
7. D. Yang, T. Chen and Z. Wang, *J. Mater. Chem. A*, 2017, **5**, 18967–18971.
8. J. Han, X. Ji, X. Ren, G. Cui, L. Li, F. Xie, H. Wang, B. Li and X. Sun, *J. Mater. Chem. A*, 2018, **6**, 12974–12977.
9. L. Zhang, X. Ji, X. Ren, Y. Ma, X. Shi, Z. Tian, A. M. Asiri, L. Chen, B. Tang and X. Sun, *Adv. Mater.*, 2018, **30**, 1800191.
10. X. Ren, G. Cui, L. Chen, F. Xie, Q. Wei, Z. Tian and X. Sun, *Chem. Commun.*, 2018, **54**, 8474–8477.
11. L. Zhang, X. Ji, X. Ren, Y. Luo, X. Shi, A. M. Asiri, B. Zheng and X. Sun, *ACS Sustainable Chem. Eng.*, 2018, **6**, 9550–9554.
12. R. Zhang, Y. Zhang, X. Ren, G. Cui, A. M. Asiri, B. Zheng and X. Sun, *ACS Sustainable Chem. Eng.*, 2018, **6**, 9545–9549.
13. D. Bao, Q. Zhang, F. Meng, H. Zhong, M. Shi, Y. Zhang, J. Yan, Q. Jiang and X. Zhang, *Adv. Mater.*, 2017, **29**, 1604799.
14. S. Li, D. Bao, M. Shi, B. Wulan, J. Yan and Q. Jiang, *Adv. Mater.*, 2017, **29**, 1700001.
15. M. Shi, D. Bao, B. Wulan, Y. Li, Y. Zhang, J. Yan and Q. Jiang, *Adv. Mater.*, 2017, **29**, 1606550.
16. J. Wang, L. Yu, L. Hu, G. Chen, H. Xin and X. Feng, *Nat. Commun.*, 2018, **9**, 1795.

17. M. Shi, D. Bao, S. Li, B. Wulan, J. Yan and Q. Jiang, *Adv. Energy Mater.*, 2018, **8**, 1800124.
18. C. Lv, Y. Qian, C. Yan, Y. Ding, Y. Liu, G. Chen and G. Yu, *Angew. Chem., Int. Ed.*, 2018, **57**, 10246–10250.
19. Y. Liu, Y. Su, X. Quan, X. Fan, S. Chen, H. Yu, H. Zhao, Y. Zhang and J. Zhao, *ACS Catal.*, 2018, **8**, 1186–1191.
20. X. Yang, K. Li, D. Cheng, W. Pang, J. Lv, X. Chen, H. Zang, X. Wu, H. Tan, Y. Wang and Y. Li, *J. Mater. Chem. A*, 2018, **6**, 7762–7769.
21. Y. Zhang, W. Qiu, Y. Ma, Y. Luo, Z. Tian, G. Cui, F. Xie, L. Chen, T. Li and X. Sun, *ACS Catal.*, 2018, **8**, 8540–8544.
22. X. Zhang, Q. Liu, X. Shi, A. M. Asiri, Y. Luo, X. Sun and T. Li, *J. Mater. Chem. A*, 2018, **6**, 17303–17306.
23. J. Han, Z. Liu, Y. Ma, G. Cui, F. Xie, F. Wang, Y. Wu, S. Gao, Y. Xu and X. Sun, *Nano Energy*, 2018, **52**, 264–270.
24. X. Li, T. Li, Y. Ma, Q. Wei, W. Qiu, H. Guo, X. Shi, P. Zhang, A. M. Asiri, L. Chen, B. Tang and X. Sun, *Adv. Energy Mater.*, 2018, **8**, 1801357.
25. W. Qiu, X. Xie, J. Qiu, W. Fang, R. Liang, X. Ren, X. Ji, G. Cui, A. M. Asiri, G. Cui, B. Tang and X. Sun, *Nat. Commun.*, 2018, **9**, 3485.
26. R. Zhang, H. Guo, L. Yang, Y. Wang, Z. Niu, H. Huang, H. Chen, L. Xia, T. Li, X. Shi, X. Sun, B. Li and Q. Liu, *ChemElectroChem*, 2018, DOI: 10.1002/celec.201801484.
27. J. Zhao, L. Zhang, X. Xie, X. Li, Y. Ma, Q. Liu, W. Fang, X. Shi, G. Cui and X. Sun, *J. Mater. Chem. A*, 2018, **6**, 24031–24035.
28. X. Ren, J. Zhao, Q. Wei, Y. Ma, H. Guo, Q. Liu, Y. Wang, G. Cui, A. M. Asiri, B. Li, B. Tang and X. Sun, *ACS Central Sci.*, 2019, **5**, 116–121.
29. R. Zhang, J. Han, B. Zheng, X. Shi, A. M. Asiri and X. Sun, *Inorg. Chem. Front.*, 2018, DOI: 10.1039/C8QI01145A.
30. H. Huang, L. Xia, R. Cao, Z. Niu, H. Chen, Q. Liu, T. Li, X. Shi, A. M. Asiri and X. Sun, *Chem. Eur. J.*, 2018, DOI: 10.1002/chem.201805523.